



Influence of SiO₂ on the structural and dielectric properties of ZnO·Bi₂O₃·SiO₂ glasses

Rajni Bala,¹ Ashish Agarwal,^{2*} Sujata Sanghi,² and S. Khasa³

¹Department of Physics, Maharshi Dyanand University, Rohtak-124001, Haryana, India, ²Department of Applied Physics, Guru Jambheshwar University of Science and Technology, Hisar-125001, Haryana, India, ³Department of Physics, Deenbandhu Chottu Ram University of Science and Technology, Murthal-131039, Haryana, India.

Received: 26-08-2014

ABSTRACT

Glasses having composition 20ZnO·(80-x)Bi₂O₃·xSiO₂ (0 ≤ x ≤ 50 mol%) were prepared by the conventional melt-quench technique. Conduction and relaxation mechanism in these glasses were studied using impedance spectroscopy in the frequency range from 10Hz to 7MHz and in the temperature range from 473K to 703 K. The complex impedance plots show depressed semicircles that shift towards origin with increase in temperature which reveals the migration of charge carrier ions in glass matrix is thermally stimulated. The ac and dc conductivities, activation energy for dc conduction (E_{dc}) and relaxation (E_τ) were extracted from the impedance spectra. The compositional variation in conductivity has been attributed to the presence of mixed glass former effect in these glasses. Similar values of E_{dc} and E_τ for each glass composition indicate that the charge carrier ions have to overcome the same energy barrier during conduction as well as relaxation processes. The perfect overlapping of normalized plots of electrical modulus on a single 'master curve' for all temperatures reveals that the conductivity relaxation occurring at different frequencies exhibit temperature independent dynamical processes. IR spectra reveals that in these glasses, Bi₂O₃ acts as both network former with [BiO₃] pyramidal units and as modifier with [BiO₆] octahedral units. The compositional dependence of density, molar volume and glass transition temperature were analyzed and correlated with the structural changes occurring in the glasses.

Keywords: Bismuth silicate glasses, FTIR, Glass transition temperature, Electrical properties, Dielectric studies.

INTRODUCTION

In the past two decades, unconventional novel oxide glasses formed with network formers such as Bi₂O₃, PbO and Ga₂O₃ have been attractive materials of research for their manifold technological applications.¹ Bismuth oxide based glasses possess high thermal stability, durability, composition tunability, high refractive index, long infrared cutoff and high nonlinear susceptibility which make them promising candidates for photonic applications such as optical switches, broadband amplification devices and optical waveguides.²⁻⁸ Due to large values of energy band gap, dielectric permittivity and photoconductivity, these

glasses are also used in gas sensors, optical coating, photovoltaic cells, microwave integrated circuits and electrochemical cells.⁹ These glasses are interesting materials for structural, optical and electrical investigations as they form stable glasses through the conventional melt quench technique even though none of the traditional glass former is added. The large polarizability and small field strength of Bi³⁺ in oxide glasses make them suitable for optical devices such as ultra-fast optical switches, optical Kerr shutters (OKS), optical isolators and environmental guidelines.¹

SiO₂ is a traditional glass former and has an extremely wide spectrum of industrial applications in its various amorphous forms.¹⁰ On the other hand, Bi₂O₃ is not a classical glass former but in the presence of conventional glass formers like SiO₂, PbO and B₂O₃, a glass network of BiO₃ and BiO₆ units may be built.¹¹ This is because the [BiO_n] polyhedra are highly distorted due to the presence of lone pair electrons. Also Bi₂O₃ possess asymmetrical structural units in the crystal state and it is possible to form bond with different lengths in distorted polyhedral. Several techniques have been employed in an attempt to identify the local environment of the different elements in bismuthate glasses. Hazra et al. have studied the properties of unconventional Bismuth-cuprate glasses which shows the glass forming ability of Bi³⁺ ions in the presence of transition

Address:

Dr. Ashish Agarwal
Department of Applied Physics, Guru Jambheshwar
University of Science and Technology, Hisar-125001,
Haryana, India
Tel: +91-1662-263384; fax: +91-1662-276240.
Email: aagju@gmail.com

Cite as: *J. Integr. Sci. Technol.*, 2015, 3(1), 6-13.

© IS Publications JIST ISSN 2321-4635

metal copper ions as $[\text{BiO}_3]$ pyramidal units.¹² Further, Batal et al. have studied the IR spectra, thermal properties and density values of $\text{Bi}_2\text{O}_3\cdot\text{SiO}_2$ glasses and found the sharing of Bi^{3+} in network glass structure as octahedral BiO_6 groups and the possibility of presence of BiO_3 units.¹³ Recently, some authors have also revealed that the participation of bismuth ions in the glass network as both octahedral BiO_6 groups and pyramidal BiO_3 groups.¹⁴⁻¹⁷ Mahaji et al. have reported that conduction and relaxation in $\text{ZnO}\cdot\text{Bi}_2\text{O}_3\cdot\text{B}_2\text{O}_3$ glasses were due to the hopping and migration of Bi^{3+} cations in their own and different local environment.¹⁸ These investigations show the effect of conventional glass former on the structural units of the unconventional glass former Bi_2O_3 . Thus, the structural role played by Bi_2O_3 in oxide glasses is very complicated and poorly understood. Due to dual behavior, bismuth ions may also influence the electrical properties of oxide glasses. The glasses containing transition metal ion such as ZnO , CdO and V_2O_5 have gained importance in recent years due to their possible applications in various technological fields.^{19,20}

Review of the literature shows that study on transport properties of glasses have been carried out due to their potential applications in different technologies like fuel cells, solid state batteries, chemical sensors, etc.²¹⁻²³ The electrical conductivity of disordered materials is caused by at least two different contributions. First being thermal activation, in which the conductivity increases with temperature according to the Arrhenius law and second is by structural change of glass with composition.²⁴ Therefore, it is interesting to study the dynamic and relaxation mechanisms of mobile ions in disordered ion conductors by interpreting the frequency dependent features in their dielectric response. The aim of the present work is focused on the structural changes induced in ternary $\text{ZnO}\cdot\text{Bi}_2\text{O}_3\cdot\text{SiO}_2$ glasses when SiO_2 replaces Bi_2O_3 content. For this a systematic study of density, molar volume, glass transition temperature and infrared spectra of all the glasses was made and the main attention is given to mid infrared region ($400\text{-}1400\text{ cm}^{-1}$) which provides the structural information. In addition to this a comprehensive overview of the electrical properties like ac and dc conductivity along with dielectric relaxation mechanism in these glasses as a function of frequency and temperature has also been studied.

EXPERIMENTAL DETAILS

Zinc bismuth silicate glasses having composition $20\text{ZnO}\cdot(80-x)\text{Bi}_2\text{O}_3\cdot x\text{SiO}_2$ (with $x = 0, 10, 20, 30, 40$ and 50 mol%) were prepared by the conventional melt-quench technique. The weighed reagent grades of ZnO , Bi_2O_3 and SiO_2 chemicals were taken to make a batch of 20 g sample. The chemicals were put in a porcelain crucible and melted in an electric furnace at $1100/1150\text{ }^\circ\text{C}$ in air for 0.5 h . During melting, the glass melt was stirred thoroughly several times to ensure homogeneity. After melting, the glass melt was poured onto a stainless-steel plate and pressed with another plate. The glass was annealed below its glass transition temperature for four hours and subsequently cooled at room temperature in the furnace. The exact composition along with the sample code of each glass is presented in Table 1. The amorphous state of the glasses was confirmed by X-ray diffraction using a Rigaku Miniflux-II diffractometer with

$\text{Cu K}\alpha$ radiation at room temperature (RT) in the 2θ range $10\text{-}80^\circ$ at scanning rate of $2^\circ/\text{min}$. The density (D) of the each sample was measured at RT using Archimede's method with xylene ($D_{xy} = 0.8645\text{ g/cm}^3$) as the buoyant liquid. The molar volume was calculated using the relation $V_M = \sum(x_i M_i)/D$, where x_i is the molar fraction and M_i is the total molecular weight of the i^{th} component. The glass transition temperature (T_g) was determined using differential scanning calorimeter (Q10, TA instrument) heated in temperature range from $473\text{-}1073\text{ K}$ in order to reach the constant combustion during measurement process, an inert nitrogen gas (N_2) atmosphere was used. The infrared transmission spectra of the glasses were recorded at RT in the range $400\text{-}4400\text{ cm}^{-1}$ by a fourier transform IR spectrophotometer (type Spectrum BX). For this, powdered glass samples were thoroughly mixed with dry KBr in the ratio of $1:20$ by weight and the pellets were formed under a pressure of $7\text{-}8$ tones to produce clear homogenous discs. The infrared transmission spectra were recorded immediately after preparing the desired discs. For dielectric measurement, samples were polished in square/rectangular shapes and silver electrodes were painted on opposite faces. The samples were then annealed at 473 K for 2 h in an electric furnace. The complex impedance data of the samples at constant voltage was measured by using an impedance gain/phase analyzer (Newton's 4th Ltd.) over a wide frequency range from 1 Hz to 7 MHz and in temperature range from 473 K to 703 K .

RESULTS AND DISCUSSION

3.1 Physical properties

X-ray diffraction (XRD) spectra of all the glasses are shown in Figure 1. All samples were found to be in glassy form with a broad hump which is a characteristic of amorphous nature. This indicates the absence of long range atomic arrangement and also the periodicity of three dimensional networks in the glasses. The density is affected by the structural softening/compactness, change in geometrical configurations, coordination numbers, cross link densities and dimensions of interstitial space of the glass. The compositional variation of density (D) as well as the transition temperature (T_g) with SiO_2 content for all the glasses are shown in Figure 2 and their corresponding values are presented in Table 1. It can be observed from the table that density decreases with decrease in Bi_2O_3 content in the ternary zinc bismuth silicate glasses. Pan et al. have reported that upto some extent, the SiO_4 tetrahedra can be

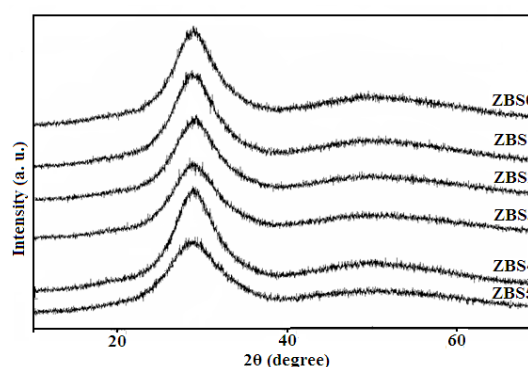


Figure 1. XRD patterns of all ZBS glasses.

Table 1. Density (D), molar volume (V_M), crystalline molar volume (V_C) and glass transition temperature (T_g) for $20\text{ZnO}\cdot(80-x)\text{Bi}_2\text{O}_3\cdot x\text{SiO}_2$ (ZBS) glasses.

| Glass Code | x (mol%) | D (g/cm^3) | V_M (cm^3/mol) | V_C (cm^3/mol) | T_g ($^\circ\text{C}$) |
|------------|----------|------------------------------|------------------------------------|------------------------------------|----------------------------|
| ZBS0 | 0 | 6.88 | 56.57 | 44.79 | 442.19 |
| ZBS1 | 10 | 6.98 | 49.93 | 42.13 | 440.52 |
| ZBS2 | 20 | 6.94 | 44.34 | 39.48 | 445.48 |
| ZBS3 | 30 | 6.90 | 38.73 | 36.82 | 450.00 |
| ZBS4 | 40 | 6.62 | 34.24 | 34.16 | 468.79 |
| ZBS5 | 50 | 5.67 | 32.88 | 31.51 | 490.68 |

incorporated in the network of more flexible structure of bismuth oxygen polyhedra $[\text{BiO}_n]$, due to more ionic nature of the Bi–O bond and hence evidence the anomalous increase in density on introduction of SiO_2 upto 10 mol% in the present glass system.²⁵ The decrease in density on further addition of SiO_2 is an expected result and can be related to the replacement of the Bi_2O_3 (atomic mass 465.98) with SiO_2 (atomic mass 60.08).

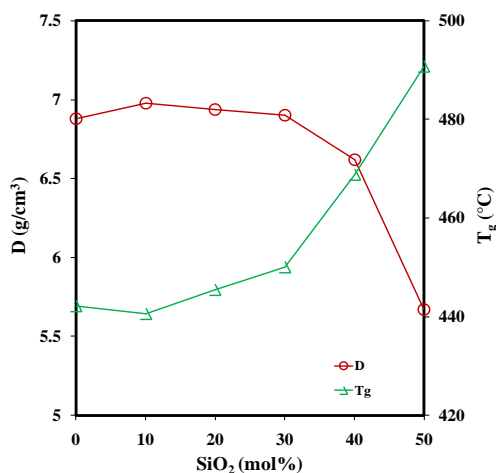


Figure 2. Compositional dependence of D and T_g for ZBS glasses.

Supercooled liquids are often called rubbers and solids are called glasses, transformation between the liquid and solid states occur over a temperature range known as glass transition temperature. The increase in T_g with the increase of SiO_2 content is due to increase in density of cross-linking of the silicate units in the glass network. The weak Bi–O–Bi cross-linkages are replaced by strong Si–O–Si cross-linkage in the glass structure which increases the cohesiveness of the network and hence the glass transition temperature. It is clearly observed from Figure 2 that variation in D and T_g is small upto $x = 30$ mol% suggesting that the topology of glass network does not change significantly for small SiO_2 content. For $x > 30$ mol%, a large decrease in density and a sharp increase in transition temperature take place suggesting high thermal stability of glass network for these compositions. This anomalous behavior of density and transition temperature at $x = 30$ mol% also suggests that a peculiar change occur in the structure of these glasses at this composition.

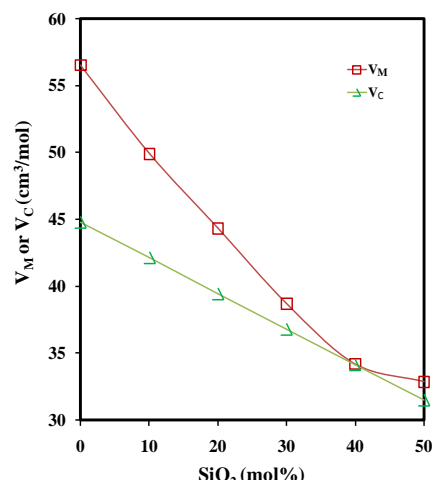


Figure 2. Compositional dependence of V_M and V_C for ZBS glasses.

The decrease in molar volume can be explained that molar volume depends on both, i.e. density and molecular weight and in the present glass system both decrease with the increase in SiO_2 at the expense of Bi_2O_3 . Also the smaller values of radii and bond length of SiO_2 as compared to that of Bi_2O_3 results in a shrinking of the free volume, thereby decreasing the overall molar volume of the glasses.

Crystalline volume of the present glasses is calculated by the formula $V_C = \sum x_i V_i$, where V_i is the molar volume of the i^{th} component in crystalline phase and their values for ZnO , Bi_2O_3 and SiO_2 are taken as 14.52, 52.36 and 25.79 cm^3 respectively. The calculated values of V_C are also included in Table 1 and the compositional dependence of V_M and V_C are shown in Figure 3 for comparison. It is clear (Figure 3) that the molar volume of the glasses is higher than that of their hypothetical mixed crystalline phase up to $x \leq 30$ mol%, and the difference between these values decreases with increase in SiO_2 content ($x > 30$ mol%) in the glass composition. The higher values of V_M compared to V_C reveals that the structure of non-crystalline counter part of these mixed crystalline phases are expanded with some excess structural volumes. This also indicates that on successive replacement of Bi_2O_3 by SiO_2 , the role of network former is replaced by SiO_4 tetrahedra which also attributes to a decrease in the number of non-bridging oxygens (NBOs).

3.2 Infrared transmission spectra

The effect of substitution of unconventional glass former (Bi_2O_3) by the conventional glass former (SiO_2) on the structural properties of zinc bismuth silicate glasses was investigated by recording their Fourier transform infrared (FTIR) spectrum in the range 400–4400 cm^{-1} . Infrared spectroscopy is one of the most useful experimental techniques which provide the easy information about the arrangement of building structural groups with respect to each other and types of bonds present in the glass.¹⁴ This technique leads to structural aspects related to both the local units constituting the glass network and the anionic sites hosting the modifying metal cations. It is accepted that the main vibrational modes appeared above 400 cm^{-1} in mid infrared range are associated with structural chain in the

glass network. These network modes are well separated from the metal ion site vibrational modes active in the far infrared region.²⁶ The studied zinc bismuth silicate glasses possess high Bi₂O₃ content ratio and thus it is expected to reflect the effect of the high mass cation of Bi³⁺ on the infrared transmission spectra.

Figure 4 depicts the IR transmission spectra from 400-1400 cm⁻¹ for all the ZBS glasses for better clarity. The mid infrared spectra of glasses containing compositional

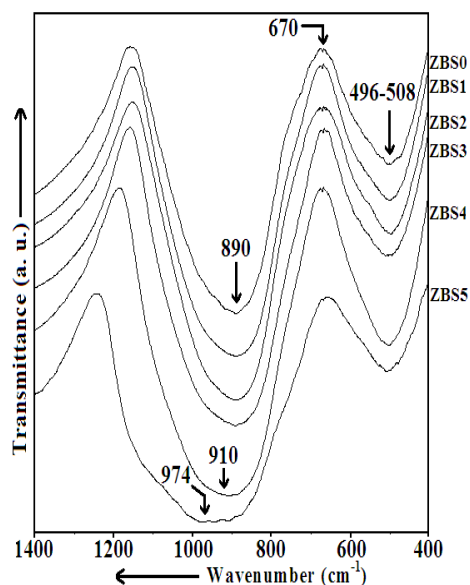


Figure 4. IR transmission spectra at RT for all the ZBS glasses (in MIR region).

variations ranging from 20ZnO·80Bi₂O₃ to 20ZnO·30Bi₂O₃·50SiO₂ (Fig. 4) show that studied glasses possess high analogues to the structure of bismuth oxide crystals and some bismuthate glasses, with Bi-O distances varying within a wide range.²⁷⁻²⁹ These Bi-O bonds are expected to have different degree of covalent or ionic character, the more covalent one corresponds to higher frequencies.²⁵ The principle and main high intense bands are observed in mid infrared region comprising of three sharp bands at 496-508 cm⁻¹, around 670 cm⁻¹ and at 890-974 cm⁻¹. A predominate band at 496 cm⁻¹ and its shifting towards higher wave number (508 cm⁻¹) with decreasing bismuth content is observed. Various authors suggest that this band originates from Bi-O bands in [BiO₆] octahedra and the shifting to higher wavenumber is due to the increase of the degree of distortions.^{13,30} Dimitriev and Mihalova have also related the shift of the band from 485 to 523 cm⁻¹ to the change in local symmetry of highly distorted [BiO₆] polyhedra, as the Bi₂O₃ content decreases.³¹ In the high wavenumber region, band around 890 cm⁻¹ for x ≤ 30 mol % is assigned to the Bi-O stretching of [BiO₃] pyramidal units.³² For x > 30 mol%, this band is broadened and shifted to higher wave number which may be related to Bi-O-Si stretched vibrations.²⁵ Some authors have observed a broad band in the wavenumber range 800-1100 cm⁻¹ which is accompanied by a broad shoulder centered at around 1200 cm⁻¹ and attributed to the stretching vibration modes of SiO₄ tetrahedral.³³ Thus, for x > 30 mol%, the band may compose of three bands but most of its intensity comes from the

stretching vibration modes of SiO₄ tetrahedra. These structural changes for x > 30 mol% are also supported by variations in the density and T_g values (Table 1).

A sharp peak around 670 cm⁻¹ observed in all the glasses is typical and is for the normal vibrations of [BiO₆] groups. Betsch et al. reported detail data on IR and Raman spectra of α-Bi₂O₃ and bismuthate phases Bi₁₂MO₂₀ having the silenite structure. With these investigations band at 670, 620, 580 and 390 cm⁻¹ in the spectrum of α-Bi₂O₃ were interpreted as vibrations of Bi-O bonds of different bond lengths in the distorted BiO₆ polyhedra.³⁴ The absorption at region 840 cm⁻¹ is not observed in these glasses, which suggests that formation of Zn²⁺ in tetrahedral coordination (i.e. ZnO₄) is absent.³⁵ With decrease in the Bi₂O₃:SiO₂ ratio a systematical change in both bands at 496 cm⁻¹ and at 890 cm⁻¹ is observed. This systematical change in these bands can be explain as: firstly, when Bi₂O₃:SiO₂ < 1, there is practically no change in the integrated ratio between the band near 890 cm⁻¹ and the band near 496 cm⁻¹ for the studied glasses in spite of a large decrease in the concentration of Bi₂O₃. At Bi₂O₃:SiO₂ = 1, intensity of the band at 496 cm⁻¹ increases while that of 890 cm⁻¹ band decreases. These results indicate that on addition of SiO₂ at the expense of Bi₂O₃ leads to a progressive conversion of BiO₃ units into BiO₆ units. Thus, in the present system Bi₂O₃ act as network modifier with BiO₆ octahedral units for all the samples and as glass former with BiO₃ pyramidal units for glass samples with x = 0, 10, 20 and 30. The observed behavior is at variance with the results reported earlier by Durga and Veeraiah who found the presence of BiO₆ units only upto composition with x = 12.³⁶ For Bi₂O₃:SiO₂ > 1 decrease in intensity of 496 cm⁻¹ band and more broadening of 890 cm⁻¹ band shows that the formation of SiO₄ units are dominated at this particular composition.

3.3 Electrical properties

Any intrinsic property that influences ion dynamics in disordered ion conducting solids is quite well studied through impedance spectroscopy (IS) by electrical relaxation measurements. IS is characterized by measurement and analysis of some or all the macroscopic complex quantities

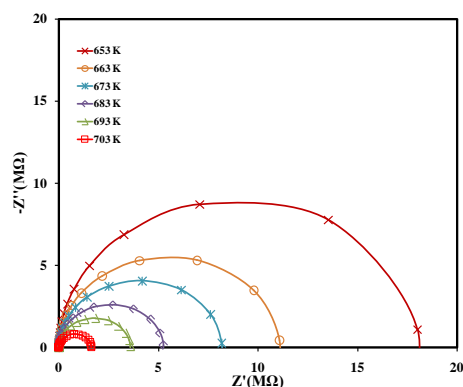


Figure 5. Experimental Nyquist plots for ZBS1 glass sample at different temperatures.

such as impedance (Z*), admittance (Y*), conductivity (σ*), electric modulus (M*) and permittivity (ε*). For analysis and interpretation of the obtained data, electrical conductivity can be described by means of frequency

Table 2. Dc and ac conductivity (σ_{dc} , σ_{ac}), activation energy for dc conduction (E_{dc}) and relaxation (E_r), power law exponent (s), dielectric loss ($\tan \delta$), relaxation time (τ_{M^r}) and stretched exponential parameter (β) for $20\text{ZnO} \cdot (80-x)\text{Bi}_2\text{O}_3 \cdot x\text{SiO}_2$ (ZBS) glasses.

| Glass Code | σ_{dc} (at 673K) (Sm^{-1}) | E_{dc} | σ_{dc} (at 673 K, 10 kHz) (Sm^{-1}) | s (at 673 K) | $\tan \delta$ (at 673K, 10 kHz) | E_r | τ_{M^r} (at 693 K) (s) | β |
|------------|--|----------|---|----------------|---------------------------------|-------|-----------------------------|---------|
| ZBS0 | 2.83×10^{-5} | 1.32 | 2.83×10^{-5} | 0.26 | 0.018 | 1.32 | 5.89×10^{-4} | 0.81 |
| ZBS1 | 8.60×10^{-6} | 1.44 | 1.80×10^{-5} | 0.38 | 0.011 | 1.46 | 1.77×10^{-3} | 0.81 |
| ZBS2 | 5.70×10^{-6} | 1.55 | 1.72×10^{-5} | 0.44 | 0.006 | 1.56 | 4.03×10^{-3} | 0.86 |
| ZBS3 | 3.18×10^{-6} | 1.60 | 1.11×10^{-5} | 0.52 | 0.008 | 1.60 | 4.03×10^{-3} | 0.88 |
| ZBS4 | 5.53×10^{-6} | 1.55 | 1.39×10^{-5} | 0.43 | 0.008 | 1.56 | 2.23×10^{-3} | 0.80 |
| ZBS5 | 2.29×10^{-6} | 1.65 | 1.37×10^{-5} | 0.54 | 0.004 | 1.65 | 5.30×10^{-3} | 0.90 |

dependent conductivity spectra. The experimental impedance data for ZBS1 glass sample is represented as Nyquist plots at different temperatures in Figure 5 which shows a single semicircle, indicating the single conduction mechanism.³⁷ No residual semicircle at lower frequency attributed to contact or electrode effects has been noticed, probably due to the fact that samples were finely polished. Figure 5 depicts that the centre of each semicircle is found to be depressed below the real axis, which suggests that the associated relaxation of ions is non-Debye in nature. As the temperature increases the radius of semicircular arc, corresponding to the bulk resistance of the glass samples, reduces suggesting that the migration of charge carrier ions is thermally stimulated. Similar results have been obtained for all other samples under investigation.

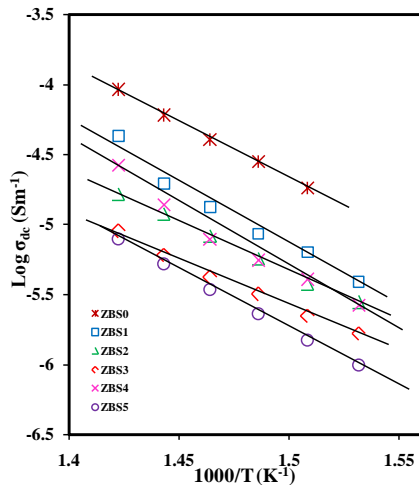


Figure 6. Reciprocal temperature dependence of dc conductivity (σ_{dc}) at different composition.

The dc conductivity, σ_{dc} , was calculated using the geometrical dimensions of the samples. The value of σ_{dc} are found to increase with increase in temperature and obeys the well known Arrhenius behavior given by:

$$\sigma_{dc} = \sigma_0 \exp\left(-\frac{E_{dc}}{kT}\right) \quad (1)$$

where σ_0 is the pre-exponential factor, which depends on composition, mobility of diffusion ions, etc. and E_{dc} is the dc activation energy of the samples. The reciprocal temperature dependence of σ_{dc} with temperature for all the glasses is shown in Figure 6. An apparent slope of one over an entire set of measurement again confirms the single conduction mechanism. The activation energy (E_{dc}) for the conduction

process was extracted from the least square fitting of these plots. The values of σ_{dc} (at 673 K) and E_{dc} are presented in Table 2. The decrease in dc conductivity and an increase in activation energy with decrease in Bi_2O_3 content upto $x = 30$ mol% is due to the mixed former effect and can be understood as follows: at high concentration of Bi_2O_3 , the network structure is largely composed of BiO_3 structural units which act as network formers. For binary zinc bismuthate glass, dc conductivity is high of the order of 10^{-5} Sm^{-1} . With successive addition of SiO_2 , the role of network former is replaced by cross linked SiO_4 tetrahedra increases the network dimensionality blocking the motion of cations and the overall mobility of the ions. FTIR spectra reveals that Bi_2O_3 acts as a network former at high concentration while it acts as a modifier at lower concentration in the present glasses. At $x = 40$ mol%, small increase in conductivity is seen which may be due to that Bi_2O_3 as network modifier (BiO_6 units) may provide more open channels to enhance the mobility of charge carriers with a consequent enhancement in electrical conductivity at this particular composition. At $x = 50$ mol%, the rate of creation of bismuth octahedral are balanced by the formation of SiO_4 tetrahedra, results in a highly cross-linked structure thus again a decrease in conductivity is seen. Therefore, when a conventional glass former is partially substituted by another conditional glass former at a constant modifier concentration in the binary-network former glasses, conductivity is found to be increased due to mixed former effect. The results of mixed former effect have also been observed in $\text{Li}_2\text{O} \cdot \text{Bi}_2\text{O}_3 \cdot \text{SiO}_2$ and $\text{ZnO} \cdot \text{Bi}_2\text{O}_3 \cdot \text{Li}_2\text{O} \cdot \text{B}_2\text{O}_3$ glass systems.^{38,39}

The measured impedance values were used to study the ac conductivity behavior of the prepared glass samples through the real part of ac conductivity. Figure 7 shows the frequency dependence of the real part of ac conductivity for the ZBS1 glass sample at various temperatures. The dispersion in conductivity is well described by the Jonscher power law (UDR) of the form⁴⁰

$$\sigma(\omega) = \sigma_{dc} + A\omega^s \quad (2)$$

where σ_{dc} is the frequency dependent dc conductivity of the sample, A is a weakly temperature dependent quantity and s is the power law exponent lies in the range ($0 \leq s \leq 1$). It is evident from Figure 7 that the frequency dependence of conductivity shows two distinct regimes: (i) the low frequency plateau regime corresponding to frequency independent conductivity, σ_{dc} , and (ii) high frequency dispersion region. The switchover from the frequency independent region to frequency-dependent region is the

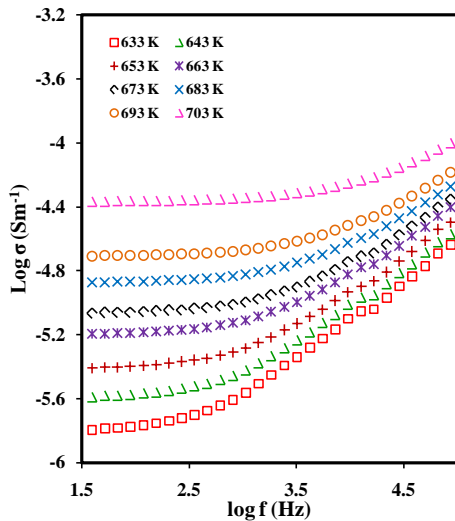


Figure 7. Frequency dependence of the conductivity, $\sigma(\omega)$, at various temperatures for ZBS1 glass.

signature of the onset of conductivity relaxation and it is shifted to higher frequency as the temperature increases. The dispersion behavior in conductivity is assigned to the microscopic nature of inhomogeneities with the distribution of relaxation processes through distribution of energy barriers in the glass.⁴¹ The values of σ_{ac} (at 673 K, 10 kHz) for all the samples are also given in Table 2. Deviation from linear variation with composition in conductivity parameters further confirms the anomalous behavior of the ZBS1 sample at $\text{Bi}_2\text{O}_3:\text{SiO}_2 = 1$. The values of dimensionless frequency exponent 's' are obtained by the slope of $\log \sigma(\omega)$ vs. $\log f$ in high frequency region and are listed in Table 2. It is observed that the value of 's' decreases with increase in temperature and is significantly lower than unity. The values are found to be material dependent (Table 2) and the glasses with lower SiO_2 content have lower 's' values. Further, the exponent 's' also depends upon the dimensionality of the local conduction space and increases with increasing dimensionality.

3.4 Dielectric studies

The phase difference due to loss of energy in the sample at a particular frequency is the loss factor tangent given by $\tan \delta = \epsilon''/\epsilon'$, where ϵ' and ϵ'' are the real and imaginary parts of the dielectric permittivity, respectively. The contribution to the dielectric loss is mainly attributed to thermally activated relaxation of freely rotating dipoles where thermal energy is the only type of relaxation and at higher temperatures it is due to electrical conduction with hopping motion of ions. The values of $\tan \delta$ (at 673K, 10 kHz) are included in Table 2. The frequency dependence of $\tan \delta$ at different temperatures for the ZBS1 glass sample is shown in Figure 8. It should be noted from this figure that $\tan \delta$ is situated in the low frequency region, where dc conductivity dominates. The temperature dependence of $\tan \delta$ at different frequencies is also shown in the insert of Figure 8 which shows that the dielectric losses at higher frequency are much lower than those occurring at lower frequency. This kind of frequency dependence of $\tan \delta$ is typically associated with losses by conduction or movement of charge carriers throughout the glass network, creating conduction losses. Consequently,

dielectric losses for samples with higher electrical conductivity are higher than for the samples having low electrical conductivity.

The electrical modulus formalism has also been employed to the IS data for a better description of the dynamic processes in the present glass system. This formalism is predominantly appropriate to identify phenomena such as electrode polarization and bulk phenomenon such as average conductivity relaxation times.⁴² The dielectric modulus is defined as $M^*(\omega) = 1/\epsilon^* = M'(\omega) + jM''(\omega)$ and its dependence on frequency is given by⁴³

$$M^*(\omega) = \frac{1}{\epsilon_\infty} \left[1 - \int_0^\infty e^{-i\omega t} \left(-\frac{d\phi}{dt} dt \right) \right] \quad (3)$$

Where ϵ_∞ is the dielectric constant at high frequency and $\phi(t)$ is the conductivity relaxation function which evolves the electric field within the material. The real ($M'(\omega)$) and imaginary ($M''(\omega)$) parts of dielectric modulus as a function of frequency at various temperatures for ZBS1 glass sample are shown in Figure 9. The behavior of dielectric modulus is qualitatively similar for all other glass samples under investigation. The real part of electric modulus $M'(\omega)$ exhibits very small values at lower frequencies barring the ease of migration of conducting ions. As the frequency is increased, $M'(\omega)$ shows a dispersion tending to M_∞ at higher frequencies. It can be assumed that in high frequency region the electric field changes so rapidly that the ions can move only within their potential wells.⁴⁴ As a result mobile ions have been frozen into the glass structure and make the glass

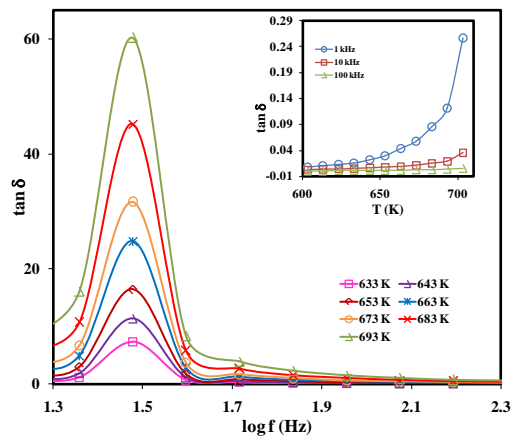


Figure 8. Frequency dependence of the dielectric loss ($\tan \delta$) at various temperatures for ZBS1 glass sample. Insert: temperature dependence of $\tan \delta$ at different frequencies.

stiffer in this frequency region and $M'(\omega)$ goes to M_∞ .⁴⁵ The imaginary part of electric modulus, $M''(\omega)$ (Fig. 9) show an asymmetric maximum at the dispersion region of $M'(\omega)$. The electrode polarization effects can be avoided since the electrical modulus peak, $M''_{\max}(\omega)$, shifts to higher frequency. The $M''(\omega)$ plots show a maximum at a characteristic frequency, known as relaxation frequency, $f_{M''}$. Figure 9 describes two relaxation regions: the low frequency side of $M''_{\max}(\omega)$ represents the range of frequencies in which charge carriers are mobile over long distances and associated with hopping conduction. The high frequency side of the $M''_{\max}(\omega)$, represents the range of frequencies in which the charge carriers are spatially confined to their

potential wells, being mobile over short range distances and associated with the relaxation polarization processes.⁴⁶ Thus, the peak frequency $f_{M''}$ is an indication of the transition from long range to short range mobility. The relaxation time $\tau_{M''}$ can be extracted from $f_{M''}$ ($=1/2\pi\tau_{M''}$). The values of $\tau_{M''}$ at 693 K for all the glasses are presented in Table 2. The reciprocal temperature dependence of $\tau_{M''}$ satisfies the Arrhenius relation represented by $\tau_{M''} = \tau_0 \exp(E_\tau/kT)$. The activation energy for relaxation process (E_τ) has been determined from the slope of the plots between $\log \tau_{M''}$ vs. $1000/T$. Further, very close values of E_{dc} and E_τ for each glass composition (Table 2) indicate that the ions have to overcome the same energy barrier during conduction as well as relaxation processes. Mostly, for disordered materials field relaxation function is given as stretched exponential function also known as the Kohlrausch–Williams–Watts (KWW) function^{47,48}

$$\phi(t) = \phi(0) \exp\left[-\left(\frac{t}{\tau}\right)^\beta\right] \quad (4)$$

where β is the Kohlrausch stretched exponent, giving the extent of non-exponentiality which measures the degree of correlation between ions in ionic transport. A completely uncorrelated motion of mobile ions i.e. Debye type relaxation occurs when β tends to approach one. It was considered that the stretched exponential is a manifestation of distribution of relaxation times.⁴⁹ Alternatively, an approach pioneered by Ngai and Jain attempts to attribute this phenomenon to the stretching of a single primitive relaxation time by interaction with other relaxing species.⁴⁹ The β parameter has been evaluated using the full width at half maximum value of $M''(\omega)$ peaks and is found to be vary from 0.81–0.90 for different glass samples and are

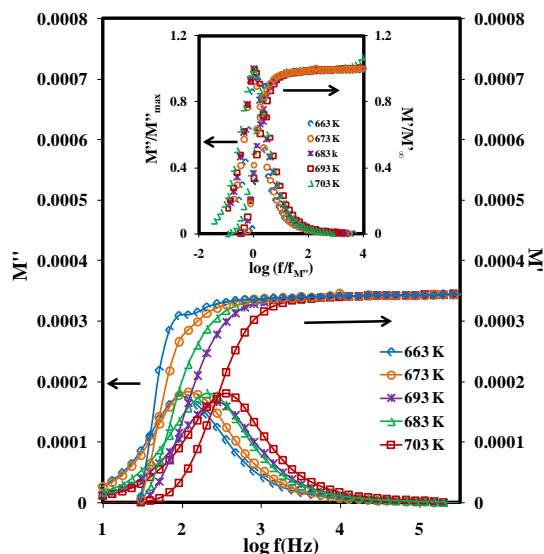


Figure 9. Frequency dependence of the real (M') and imaginary (M'') parts of modulus isotherms for ZBS1 glass at various temperatures. Inset: normalized plots of electrical modulus against normalized frequency ZBS1 glass.

temperature independent. These values suggest less deviation from the Debye ($\beta = 1$) values. The temperature independent nature of the β value is also substantiated from the superimposed plots of M''/M''_{\max} vs. $\log(f/f_{M''_{\max}})$ shown in inset of Fig. 9. Similar scaling behavior is also observed for

all other ZBS glasses. The perfect overlapping of all the curves on a single ‘master curve’ for all temperatures reveals that the conductivity relaxation occurring at different frequencies exhibit temperature independent dynamical processes.⁴⁰

CONCLUSIONS

Zinc bismuth silicate glasses having composition $20\text{ZnO} \cdot (80-x)\text{Bi}_2\text{O}_3 \cdot x\text{SiO}_2$ (with $x = 0, 10, 20, 30, 40$ and 50 mol%) were prepared by the conventional melt-quench technique. The presence of broad band in XRD pattern demonstrates the amorphous nature of all the samples. Density of these glasses decreases while T_g increases with increase in SiO_2 content and can be related to the replacement of weak Bi–O–Bi cross-linkages by strong Si–O–Si cross-linkage in the glass structure. Decrease in molar volume with decrease in Bi_2O_3 content is due to the smaller values of radii and bond length of SiO_2 as compared to that of Bi_2O_3 results in a shrinking of the free volume, thereby decreasing the overall molar volume of the glasses. The FTIR spectra were recorded in the range $400\text{--}4400\text{cm}^{-1}$ in order to obtain information about the competitive role of Bi_2O_3 and SiO_2 in the formation of glass network. From the analysis of these spectra it is found that in these glasses, Bi_2O_3 act as network modifier with BiO_6 octahedral units for all the samples and as glass former with BiO_3 pyramidal units for glass samples with $x = 0, 10, 20$ and 30 . The formation of Zn^{2+} in tetrahedral co-ordination (i.e. ZnO_4) was not observed. The dc conductivity followed Arrhenius law and decrease with increase in SiO_2 content. This may be attributed to that with increase in SiO_2 content, the role of network former is replaced by SiO_4 tetrahedral increasing the dimensionality and hence blocking the motion of cations, and overall mobility of the ions. The increase in conductivity at $x = 40$ mol % is due to the presence of mixed glass former effect of Bi_2O_3 in these glasses. The activation energies for conduction and relaxation were found to have almost similar values for these glasses, which indicate that the charge carrier ions overcome the same energy barrier while conducting as well as when relaxing. The perfect overlapping of normalized plots of electrical modulus on a single ‘master curve’ in the studied temperature range reveals that the conductivity relaxation mechanism is temperature independent.

Acknowledgements

Authors are thankful to CSIR, New Delhi for providing financial support. One of the authors (Rajni Bala) is thankful to CSIR, New Delhi for providing SRF (No. 09/752(0018)/2008-EMR-I).

REFERENCES

1. S. Bale, N. Srinivasan Rao, S. Rahman. Spectroscopic Studies of $\text{Bi}_2\text{O}_3\text{--Li}_2\text{O--ZnO--B}_2\text{O}_3$ Glasses. *Solid State Sci.* **2008**, 10, 326-331.
2. L. Baia, R. Stefan, W. Keifar, S. Simon. Structural characteristics of $\text{B}_2\text{O}_3\text{--Bi}_2\text{O}_3$ glasses with high transition metal oxides content. *J. Raman Spectrosc.* **2005**, 3, 262-266.
3. S. Simon, M. Todea. Spectroscopic study on iron doped silica bismuthate glasses and glass ceramics. *J. Non-Cryst. Solids.* **2006**, 352, 2947-2951.
4. T. Inoue, T. Honma, V. Dimitrov, T. Komatsu. Approach to thermal properties and electronic polarizability from average single bond

- strength in ZnO-Bi₂O₃-B₂O₃ glasses. *J. Solid State Chem.* **2010**, 183 3078-3085.
5. A. Dutta, A. Ghosh. Structural and optical properties of lithium barium bismuthate glasses. *J. Non-Cryst. Solids* **2007**, 353, 1333-1336.
 6. Y. B. Saddek, E. R. Shaaban, E. S. Moustafa, H. M. Moustafa. Spectroscopic properties, electronic polarizability, and optical basicity of Bi₂O₃-Li₂O-B₂O₃ glasses. *Physica B.* **2008**, 403, 2399-2407.
 7. I. Ardelean, S. Cora, R. C. Lucacel, O. Hulpus. EPR and FT-IR spectroscopic studies of B₂O₃-Bi₂O₃-MnO glasses. *Solid State Sci.* **2005**, 7, 1438-1442.
 8. S. Khata, M. Dahiya, Structural Investigations of Lithium Vanadate Bismuth-Borate Glasses, *Journal of Integrated Science and Technology* **1** (1), 44-47
 9. T. Hyodo, E. Kanazawa, Y. Takao, Y. Shimizu, M. Egashira. H₂ Sensing Properties and Mechanism of Nb₂O₅-Bi₂O₃ Varistor-Type Gas Sensors. *Electrochem.* **2000**, 68, 24-31.
 10. G. H. Beall. Design and properties of glass-ceramics. *Ann. Rev. Mat. Sci.* **1992**, 22, 91-119.
 11. W. H. Dumbaugh. Heavy metal oxide glasses containing Bi₂O₃. *Phys. Chem. Glasses.* **1986**, 27, 119-123.
 12. S. Hazra, A. Ghose. Structure and properties of nonconventional glasses in the binary bismuth cuprate system. *Phys. Rev. B.* **1995**, 51, 851-856.
 13. F. H. El Batal. Gamma ray interaction with bismuth silicate glasses. *Nucl. Inst. Meth. Phys. Res. B.* **2007**, 254, 243-253.
 14. S. Sanghi, S. Duhan, A. Agarwal, P. Aghamkar. Study of structure and optical properties of Fe₂O₃-CaO-Bi₂O₃ glasses. *J. Alloys & Comp.* **2009**, 488, 454-458.
 15. N. Ahlawat, S. Sanghi, A. Agarwal, R. Bala. Influence of SiO₂ on the structure and optical properties of lithium bismuth silicate glasses. *J. Mol. Struct.* **2010**, 96, 82-86.
 16. G. Gao, L. Hu, H. Fan, G. Wang, K. Li, S. Feng, S. Fan, H. Chen. Effect of Bi₂O₃ on physical, optical and structural properties of boron silicon bismuthate glasses. *Opt. Mater.* **2009**, 32, 159-163.
 17. S. Rani, S. Sanghi, N. Ahlawat, A. Agarwal. Influence of Bi₂O₃ on thermal, structural and dielectric properties of lithium zinc bismuth borate glasses. *J. Alloys & Comp.* **2014**, 597, 110-118.
 18. K. Mahaji, R. Vaish, G. Paramesh, K. B. R. Varma. Electric transport characteristics of ZnO-Bi₂O₃-B₂O₃ glasses. *Ionic.* **2013**, 19, 99-104.
 19. D. K. Shukla, S. Mollah, R. Kumar. Influence of TiO₂ and ZnO on conductivity and dielectric properties of copper-bismuth glasses. *J. Appl. Phys.* **2007**, 101, 013708-1.
 20. L. Srinivasa Rao, M. Srinivasa Reddy, M. Rami, Reddy, N. Veeraiah. Dielectric dispersion in Li₂O-MoO₃-B₂O₃ glass system doped with V₂O₅. *J. Alloys & Comp.* **2008**, 464, 472-482.
 21. S. Sanghi, S. Rani, A. Agarwal, V. Bhatnagar. Influence of Nb₂O₅ on the structure, optical and electrical properties of alkaline borate glasses. *Mater. Chem. & Phys.* **2010**, 120, 381-386.
 22. L. F. Maia, A. C. M. Rodrigues. Electrical conductivity and relaxation frequency of lithium borosilicate glasses. *Solid State Ionics.* **2004**, 168, 87-92.
 23. R.K. Brow, C.A. Click, T.M. Alam. Modifier Coordination and Phosphate Glass Networks. *J. Non-Cryst. Solids.* **2000**, 274, 9-16.
 24. V. C. V. Gowda, R.V. Anavekar. Transport properties of Li₂O-MnO₂-B₂O₃ glasses. *Solid State Ionics.* **2005**, 176, 1393-1401.
 25. Z. Pan, D. O. Handerson, S.H. Morgan. Vibrational spectra of bismuth silicate glasses and hydrogen induced reduction effects. *J. Non-Cryst. Solids.* **1994**, 171, 134-140.
 26. C.I. Merzbacher, W.B. White. The structure of alkaline earth aluminosilicate glasses as determined by vibrational spectroscopy. *J. Non-Cryst. Solids.* **1991**, 130, 18-34.
 27. W.H. Dumbaugh, J.C. Lapp. Heavy metal oxide glasses. *J. Am. Ceram. Soc.* **1992**, 75, 2315-2326.
 28. C. Malmros. The crystal structure of α-Bi₂O₃. *Acta Chem. Scand.* **1970**, 24, 384-396.
 29. S.C. Abrahams, P.B. Jamieson, J.L. Bernstein. Crystal structure of piezoelectric bismuth germanium oxide. *J. Chem.Phys.* **1967**, 47, 4034-4041.
 30. L. Baia, R. Stefan, W. Keifer, J. Pop, S. Simon. Structural investigation of copper doped B₂O₃-Bi₂O₃ glasses with high bismuth oxide content. *J. Raman Spectroscopy.* **2002**, 303, 379-386.
 31. Y. Dimitriev, M. Mihailova. Proceeding of 16th international Congress on Glass, Madrid **1992**, 3, 293.
 32. D. Sreenivasu, V. Chandramouli. Spectroscopic and transport properties of Cu²⁺ ion doped in (40-x)Li₂O-xLiF-60Bi₂O₃ glasses. *Bull. Mater. Sci.* **2000**, 23, 509-513.
 33. J. Wong. In Borate Glasses: Structure, Applications, Plenum Press: New York, **1977**, p. 297.
 34. R.J. Betsch, W.B. White. Vibrational spectra of bismuth oxide and the silenite structure bismuth oxide derivatives. *Spectrochim. Acta A.* **1978**, 34, 505-514.
 35. S.G. Motke, S.P. Yawale, S.S. Yawale. Infrared spectra of zinc doped lead borate glasses. *Bull. Mater. Sci.* **2002**, 25, 75-78.
 36. D.K. Durga, N. Veeraiah. Composition dependence of electrical properties of ZnF₂-MO-TeO₂ glasses. *Bull. Mater. Sci.* **2001**, 24, 421-429.
 37. K. El-Egili. AC conductivity of some alkali borosilicate glasses. *J. Phys.: Condens. Mater.* **1996**, 8, 3419-3426.
 38. N. Ahlawat, S. Sanghi, A. Agarwal, N. Kishore, S. Rani. Investigation of near constant loss contribution to conductivity in lithium bismuth silicate glasses. *J. Non-Cryst Solids* **2008**, 354, 3767-3772.
 39. S. Bale, S. Rahman. Glass structure and transport properties of Li₂O containing zinc bismuthate glasses. *Opt. Mater.* **2008**, 31, 333-337.
 40. A.K. Jonscher. The 'universal' dielectric response. *Nature.* **1977**, 267, 673-679.
 41. S. Rani, S. Sanghi, A. Agarwal, N. Ahlawat. Effect of Bi₂O₃ on the dynamics of Li⁺ ions in Li₂OP₂O₅ glasses. *J. Mater. Sci.* **2009**, 44, 5781-5787.
 42. R.A. Gerhardt. Impedance and dielectric spectroscopy revisited: Distinguishing localized relaxation from long-range conductivity. *J. Phys. Chem. Solids.* **1994**, 55, 1491-1506.
 43. C. Leon, P. Lunkenheimer, K.L. Ngai. Test of universal scaling of ac conductivity in ionic conductors. *Phys. Rev.B.* **2001**, 64, 184304.
 44. S.W. Martin, A. Angell. Dc and ac conductivity in wide composition range Li₂O.P₂O₅ glasses. *J. Non-Cryst. Solids.* **1986**, 83, 185-207.
 45. A. Dutta, T.P. Sinha, P. Jena, S. Adak. Ac conductivity and dielectric relaxation in ionically conducting soda-lime-silicate glasses. *J. Non-Cryst. Solids.* **2008**, 35, 3952-3957.
 46. A. Mogus-Milankovic, A. Santic, V. Licina, D. E. Day. Dielectric behavior and impedance spectroscopy of bismuth iron phosphate glasses. *J. Non-Cryst. Solids.* **2005**, 351, 3235-3245.
 47. R. Kohlrausch. Theory of the electrical residue in the Leiden bottle. *Pogg. Ann. Phys. Chem.* **1854**, 91, 179-214.
 48. G. Williams. D. C. Watts. Non-symmetrical dielectric relaxation behaviour arising from a simple empirical decay function. *Trans. Faraday Soc.* **1970**, 66, 80-85.
 49. K.L. Ngai, R.W. Rendell, H. Jain. Anomalous isotope-mass effect in lithium borate glasses: Comparison with a unified relaxation model. *Phys. Rev. B.* **1984**, 30, 2133-2139.
 50. K.L. Ngai, H. Jain. Conductivity relaxation and spin-lattice relaxation in lithium and mixed alkali borate glasses- Activation enthalpies, anomalous isotope-mass effect and mixed alkali effect. *Solid State Ionics.* **1986**, 18, 362-367.